Biochimica et Biophysica Acta, 1060 (1991) 175–188

ADONIS 000527289100237L

BBABIO 43496

Improved UV-visible spectra of the S-transitions in the photosynthetic oxygen-evolving system

Jérôme Lavergne

Institut de Biologie Physico-Chimique, Paris (France)

(Received 1 April 1991)

Key words: Oxygen evolving system; S state; Absorption spectroscopy; Manganese; Photosystem II center

(1) The first part of this paper is devoted to methodological tests pertaining to the deconvolution of the spectra of the S-transitions from flash sequence data. (i) The spectrum and decay kinetics of 'inactive PS II centers' were analyzed, showing similarity with normal centers inhibited on the Q_B site. When this contribution is subtracted, the change on the first flash agrees with estimate of the $S_1 \rightarrow S_2$ change derived from deconvolution. (ii) Preillumination procedures in PS II (BBY) particles, aimed at modulating the initial S_0/S_1 distribution are confirmed to express deactivation towards the S_1 state, with no involvement of an 'S_{-1}' state. (iii) Elimination of semiquinone binary oscillations in BBY's is achieved by allowing total reoxidation by DCBQ after each flash. (iv) A deconvolution treatment is described, using the difference between two sequences. This method allows a determination of the initial S_0/S_1 distributions that cross-checks the conclusions (ii). (v) Oscillations of the amplitude of the ms-phase of the 295 nm absorption changes are shown to differ significantly from those corresponding to the S-transitions. This phase is expected to reflect predominantly the O_2 release reaction, with slight deviations due to other transitions. Deconvolution results are in satisfactory agreement with this prediction. (2) The upshot of this work is to present improved spectra of the S-transitions. The basic features that were previously established with different material and deconvolution method are confirmed: negligible UV change on $S_0 \rightarrow S_1$ and significantly different spectra for the two other transitions. A shoulder around 350 nm on the $S_1 \rightarrow S_2$ spectrum and a secondary peak in the same region for the $S_2 \rightarrow S_3$ spectrum are now resolved. The $S_0 \rightarrow S_1$ step causes an electrochromic shift in the blue region, with direction opposite to $S_1 \rightarrow S_2$. Interpretation of these results is discussed.

Introduction

The existence of an integrated 'oxygen-evolving complex' (OEC) on the donor side of Photosystem II was originally inferred by Joliot and Kok [1] from their works on oxygen evolution under flash illumination that revealed sequential accumulation of the four oxidizing equivalents involved in the splitting of two water molecules. A formal description is given by the Kok cycle:

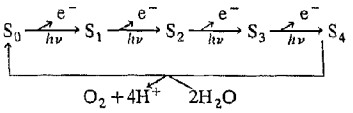

in which the S-states are successive oxidation states of the system. On a minutes time-range, S_0 and S_1 are the only stable states in the dark, while S_2 and S_3 become re-reduced towards S_1. State S_4 is highly unstable, decaying towards S_0 in a millisecond-reaction accompanied by release of molecular oxygen. Under excitation with short saturating flashes, the cycle advances by one step in most centers, except for randomly distributed fractions that undergo no transition (probability α of 'misses') or two transitions on a single flash (probability β of 'double hits').

Abbreviations: BBY, granal membrane preparation according to Berthold et al. [10]; PS, Photosystem; DCBQ, 2,5-dichloro-*p*-benzoquinone; DCMU, 3-(3,4-dichlorophenyl)-1,1-dimethylurea; FCCP, carbonylcyanide p-trifluoromethoxy-phenylhydrazone; OEC, oxygen evolving complex.

Correspondence: J. Lavergne, Institut de Biologie Physico-Chimique, 13 rue Pierre et Marie Curie, 75005 Paris, France.

The underlying molecular gears of this system have been the object of extensive investigations in the recent years (see reviews [2,3]). From biochemical and spectroscopic evidence, it has become clear that a key role is played by a cluster of four manganese atoms that probably shapes the catalytic site for water splitting and participates in oxidant accumulation. However, only in the case of the $S_1 \rightarrow S_2$ transition does strong experimental support exist for the direct involvement of Mn. Indeed, both EPR and X-ray spectroscopy suggest that an Mn(III) to Mn(IV) oxidation occurs at this step. UV-visible absorption spectroscopy should provide important additional information as to the nature of the S-states. However, conflicting results have been reported in this area [4–9], which has reduced their potential usefulness.

The first detailed study of the absorption changes associated with the successive oxidation steps of the OEC was that of Dekker and co-workers [4]. A conclusion of this work was that of identical spectral changes occurring on $S_0 \rightarrow S_1$, $S_1 \rightarrow S_2$, $S_2 \rightarrow S_3$ (with the accumulated change being reversed on the $S_3 \rightarrow (S_4 \rightarrow) S_0$ oxygen-evolving transition: thus a '1, 1, 1, −3' pattern). This suggested an identical chemistry going on in each of these steps as well: the authors proposed an Mn(III) → Mn(IV) reaction occurring successively on three Mn atoms (thus, state S_0 would include three Mn(III), S_1 two Mn(II) and one Mn(IV), and so forth). The spectral shape that was found in the near-UV could indeed be ascribed to a change in a metal-to-ligand charge-transfer band occurring upon Mn oxidation, as was observed in model compounds.

The present author's investigations on the spectra of the S-transitions turned out to be in significant disagreement with the 1, 1, 1, −3 model. This was first on qualitative grounds showing that, in the 295 nm region (where signals from the quinone acceptors are negligible), the change at the second step ($S_1 \rightarrow S_2$) had to be significantly larger than those at the first and third ones [5]. I then developed a method for eliminating undesirable perturbation from the acceptor side (in an algal mutant devoid of PS I), that allowed quantitative determination of the spectra [6]. By contrast with the 1, 1, 1, −3 pattern, different spectra were resolved for each transition and the major discrepancy with Dekker's conclusions was the finding of no significant change in the near-UV for the $S_0 \rightarrow S_1$ step. In recent publications, Dekker [8] and Van Gorkom [9] maintained their original standpoint.

The first part of this paper (that may be skipped by readers who are not primarily interested in these technical aspects) is devoted to re-examining the optical data and the validity of methods used for deriving the individual spectra of the S-transitions. Sensitive questions such as the determination of the initial S_0/S_1 distribution and its modulation through flash preillumination have been submitted to detailed tests and cross-checking. The second part of the paper presents and discusses the spectra obtained with 'BBY' particles, allowing a somewhat improved resolution with respect to the algal cells used in Ref. 6. This study results in clear confirmation of my previous findings and in the obtaining of better resolved spectra for the S-transitions.

Materials and Methods

Biological materials

The double mutant S-56 of *Chlorella sorokiniana* was used as previously described [6], after a pre-treatment with *p*-benzoquinone for maintaining a completely oxidized state of the pool of PS II acceptors under dark adapted conditions. This strain is devoid of PS I reaction centers and lacks most of the peripheral pigment antenna.

PS II-enriched membrane fragments ('BBY particles') from spinach were prepared as in Ref. 10, omitting the second Triton incubation step. A simplified preparation was also sometimes used in which the membrane fragments were pelleted in a single centrifugation following the Triton incubation, with no significant change in the results. The amount of photo-oxidizable P-700 was found negligible in all cases and no photo-oxidation of cytochrome-*f* could be detected. The particles were stored frozen and diluted for use at a concentration of 12.5 μg chlorophyll/ml in a medium containing 0.3 M sucrose, 10 mM NaCl, 5 mM $MgCl_2$, 5 mM $CaCl_2$ and 25 mM Mes (pH 6.5). Other additions are further described in the text.

Detection of absorption changes

This was achieved as previously described [6], using the Joliot-type spectrophotometer [11,12]. This machine samples the absorption at discrete times, using relatively intense monochromatic flashes of a few microseconds duration that ensure high signal-to-noise ratio while keeping the actinic effect negligible. Saturating xenon flashes of a few microseconds duration were used as actinic illumination through a broad-band red filter.

Deconvolution of raw data

I outline here only the general features of the problem, while specific procedures will be described later. Assuming validity of the Kok model (as described in the introduction), the S-state distribution during a sequence of flashes is entirely predictible from the knowledge of three parameters: the probabilities for misses and double-hits (α and β, respectively) and the initial (dark-adapted) distribution of the two stable states, S_0 and S_1. I denote by σ the initial S_0 concentration: thus, $S_1 = 1 - \sigma$, taking 1 for the total concen-

tration of the OEC. The set α, β, σ determines the values $S_i(n)$ where i labels the state (0 to 3) and n the flash number. Indeed, knowing the S distribution after flash $n-1$, one can compute it after flash n:

$$S_i(n) = \alpha S_i(n-1) + (1-\alpha-\beta)S_{i-1}(n-1) + \beta S_{i-2}(n-1) \quad (1)$$

where the i's are taken modulo 4.

Let us now call ϵ_i the extinction coefficient of state i. Then the absorbance after flash n is:

$$A(n) = \sum_{i=0}^{3} \epsilon_i S_i(n) \quad (2)$$

The absorbance *change* caused by flash n is thus:

$$\Delta A(n) = \sum_{i=0}^{3} \epsilon_i (S_i(n) - S_i(n-1)) \quad (3)$$

Using $\Sigma S_i = 1$ and straightforward algebra, this is rewritten as:

$$\Delta A(n) = \sum_{i=0}^{2} e_i T_i(n) \quad (4)$$

in which the e_i terms denote the differential extinction coefficients $e_i = \epsilon_{i+1} - \epsilon_i$ and the T terms are transition weights as given below:

$$T_0(n) = S_0(n-1) - S_0(n) \quad (5a)$$

$$T_1(n) = T_0(n) + S_1(n-1) - S_1(n) \quad (5b)$$

$$T_2(n) = T_1(n) + S_2(n-1) - S_2(n) \quad (5c)$$

Therefore, Eqn. 4 corresponds to a linear system with three unknowns (e_0, e_1 and e_2). The left-hand-side values $\Delta A(n)$ (absorption changes upon each flash of a series) are experimentally measured, while the T values are computed from Eqns. 5 and 1, knowing the three Kok parameters α, β and σ. Only three equations (three flashes) are strictly required for solving the system, while using more flashes and an appropriate least-squares method [6] will improve the treatment of noisy data.

Besides the obvious (and difficult) requirement of obtaining reliable $\Delta A(n)$ data free of extraneous contributions, the basic problem is the determination of the Kok parameters. It was shown by Lavorel [13] that α and β can be computed from any Kokian sequence, irrespective of the initial concentrations and particular weighting of the S-states in the experimentally observed response. Thus any set of 7 consecutive $\Delta A(n)$ can be used to compute α and β in the absence of any information on the ϵ values and σ (using more flashes will of course improve the reliability). This method was used here as described earlier [6]. In that previous work, the problem of determining σ (the initial S_0 concentration) was solved by preparing dark-adapted states in which σ could be predicted from appropriate flash preillumination procedures preceding deactivation. This took advantage of the fact that states S_2 and S_3 deactivate towards S_1, leaving unaffected the amount of S_0 [1]. Thus a one flash preillumination will leave a fraction α of the initial S_0 amount in the same state. Since α is on the order of 10% and S_0 usually about 25% this procedure results in 97–98% of the centers in the S_1 state after deactivation, with little incidence of the precise initial S_0 concentration. Giving three more preillumination flashes on this S_1-rich ($\sigma \approx 0.025$) state results in a S_0-rich state in which the new σ can be computed from the previous one with the knowledge of α and β. This treatment, which relies on the assumption of 100% deactivation of S_2 and S_3 towards S_1, in the presence of FCCP (used to accelerate deactivation), was questioned by Dekker [8], so that I resorted here to an alternative method, to be described in the next section, that still uses preillumination procedures, but allows an *experimental determination* of σ irrespective of any assumption concerning the deactivation mechanism.

Methodological tests

Contribution of 'inactive centers' on the first flash

When extracting the extinction coefficients of the S-transitions from flash sequence data, most of the useful information is contained in the first few flashes, before too much mixing of the individual states has occurred. It is thus unfortunate that an additional absorption change is present on the first flash (denoted FF in Ref. 6), precluding the direct use of the first flash signal in the deconvolution. My first topic will be to show how this additional change can be estimated and subtracted in order to restore the information pertaining to the S-transitions. In addition, this study will shed light on the nature of the 'inactive PS II centers' [14,15] which are at the origin of the additional signal. The experiments described in this section were carried out using the same mutant strain (S-56) of *Chlorella sorokiniana* as in previous work [5–7], while the rest of the paper will be devoted to results obtained with BBY particles from spinach.

In Ref. 6, a first spectrum of the FF signal was obtained by treating it as an additional unknown in the deconvolution of the S-changes, assuming its contribution on the first flash of a sequence to be constant irrespective of the preillumination/deactivation procedures that were used for setting the initial S_0/S_1 distribution. This spectrum was found very similar to that of the $S_1Q_A \rightarrow S_2Q_A^-$ transition, except in the blue region (absence of the 430 nm trough). However, discrepancy in this region may have been caused by an

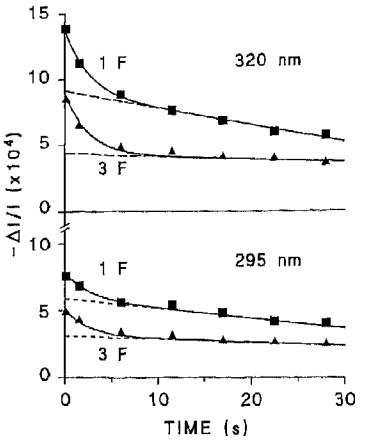

Fig. 1. Time-courses of the absorption changes at 295 and 320 nm following one flash or a group of three flashes (spaced 50 ms apart) in S-56 cells. The algae were pretreated with benzoquinone as described in the Methods section and used in the presence of 0.5 mM of the ionophore dicyclohexyl-18-*crown*-6 (no FCCP was present). The dashed line is an extrapolation of the slower phase, showing the amplitude of the faster phase ($t_{1/2} \approx 1$ s).

inaccurate correction of the photo-oxidation signal of cytochrome *b*-559 induced by the presence of FCCP in these experiments. If such was the case, then the FF signal could be ascribed to centers that do not transfer electrons to the secondary quinone acceptor Q_B, but are otherwise normal. In other words, these centers would behave like DCMU-inhibited centers. This hypothesis can be tested, since centers of that type are expected to back-react ($S_2Q_A^- \rightarrow S_1Q_A$) with a half-time of 1–2 s. We thus searched whether a decay component was occurring in this time range. In the experiment of Fig. 1 the kinetics of the absorption changes at 295 nm and 320 nm were recorded after one flash or a group of three flashes. A phase with $t_{1/2} \approx 1$ s is apparent, superimposed on a slower decay which is more pronounced in the one-flash experiments, presumably reflecting the $S_2Q_B^- \rightarrow S_1Q_B$ recombination in normal centers. At a given wavelength, the amplitude of the 1 s phase is similar after one flash or a group of three flashes, thus not related to the functional OEC. Spectral data on the amplitude of this phase are shown in Fig. 2 (open squares) and may be compared with the $S_1Q_A \rightarrow S_2Q_A^-$ spectrum (solid circles) obtained in the presence of DCMU. Both spectra are identical within experimental accuracy; in particular, the 430 nm trough is present in the spectrum of the 1 s decay. These findings thus fully support the interpretation of inactive centers like 'DCMU-inhibited' centers. Also in agreement with this view, I found (in unpublished work with E. Leci) that the 1 s phase was suppressed in the presence of millimolar hydroxylamine and replaced by a slower decay with $t_{1/2} \approx 20$ s. This confirms the back-reaction mechanism, but also indicates that the blocking of secondary electron transfer on the acceptor side is not as stringent in inactive centers as in normal centers in the presence of DCMU.

From the knowledge of the shape of the spectrum associated with inactive centers (identical to the change measured in the presence of DCMU), one can estimate (and subtract) their contribution at any wavelength, if some reference wavelength can be found where no other signal is superimposed. We will show that the 550 nm change can be used to that end. Fig. 3 shows a set of absorption changes in S-56 cells during a series of flashes. The FCCP concentration was halved and the flashing frequency doubled with respect to our previous conditions [6]. This renders negligible the extent of deactivation between flashes and the associated cytochrome *b*-559 photo-oxidation. In the left-hand part of the figure were plotted the absorption signals measured at 25 ms after each flash at the peak (540 nm) and trough (550 nm) wavelengths of the C-550 change which is known to be an indicator of Q_A reduction. At 550 nm, one observes a step change on the first flash, followed by a linear decrease. This is readily interpreted as formation of Q_A^- in inactive centers on the first flash, followed by progressive accumulation of Q_A^- in active centers accompanying the reduction of the plastoquinone pool (the S-56 strain is devoid of PS I centers). A similar pattern is observed at 540 nm, with superimposition of an oscillating component. The presence of an oscillating pattern ar 540 nm but not at 550 nm agrees with the previous finding [6] of a significant amplitude of the S-spectra in the green region, that falls off between 540 and 550 nm, and

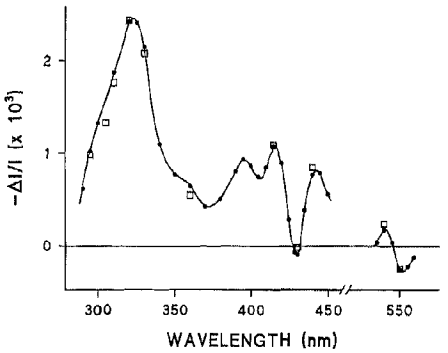

Fig. 2. A comparison between the amplitude of the 1 s decay phase and the spectrum of the flash-induced change in the presence of DCMU. The solid circles and line show the absorption change sampled in the 50–100 ms range after a flash in the presence of $2 \cdot 10^{-5}$ M DCMU, averaging data from a series of 11 flashes (20 s apart) where the first one (that may contain an $S_0 \rightarrow S_1$ contribution) was discarded. The amplitude of the 1 s phase (open squares) was determined as the absorption difference between 50 ms and 5 s after a flash, averaging series of ten flashes spaced 20 s apart. These data were normalized at 320 nm on the value of the first spectrum.

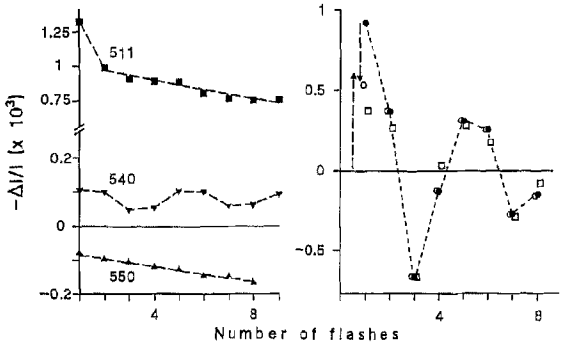

Fig. 3. Absorption changes during a series of flashes spaced 25 ms apart in S-56 cells. The suspension medium contained 0.25 μM FCCP. Before starting the flash series, the algae were preilluminated for 200 ms with continuous red light, deactivated for 20 s, illuminated by one flash and again deactivated for 20 s. The continuous light period causes equidistribution of the Q_B and Q_B^- forms [6] while the flash preillumination prepares an S_1-rich state. Left-hand panel: The 511 nm change was measured at 75 μs after each flash and plotted with respect to the absorption level taken immediately before the flash. The 511 nm datapoint on the second flash is indicative of the number of active centers involved in oxygen evolution. Its value (taken from the dashed line) is 0.975. The 540 nm and 550 nm changes were measured at 25 ms after each flash (i.e., immediately before the next one) and plotted with respect to the dark-adapted baseline recorded before starting the flash series. The amount of 'inactive centers' can be estimated from the step change at 550 nm on the first flash. Its value (taken on the dashed line) is -0.085. Right-hand panel: The 295 nm change was measured at 25 ms after each flash with respect to the absorption level preceding the flash (solid circles). A constant offset upon each flash (an absorption increase equal to 0.075) was measured separately (as in Ref. 6) and subtracted. The open circles show the fit of these data (not using the first flash) with $\alpha = 0.104$, $\beta = 0.04$ and initial $S_0 = 0.026$ (expected from the flash preillumination). The following extinction coefficients were obtained for the successive S-transitions: $e_0 = 0.080$, $e_1 = 0.586$ and $e_2 = 0.510$. The open squares are the simulated sequence taking $e_0 = e_1 = e_2$ (Dekker's model) with the same Kok parameters and normalization on the third flash. The triangles show two ways of restoring the first flash change, using the data of the left-hand panel. The downward arrow corresponds to a subtraction of the contribution of inactive centers, calibrated through the 550 nm change and using the spectrum of Fig. 2. In the latter, the (295 nm)/(550 nm) ratio is -4.01, thus the correction is $0.085 \times 4.01 = 0.341$. The upward pointing arrow is an estimate of the $S_1 \rightarrow S_2$ contribution of active centers on the first flash, estimating their amount through the 511 nm change (0.975). The ratio of the 295 nm change due to $S_1 \rightarrow S_2$ with respect to the 511 nm change at 75 μs was obtained in a separate experiment in the presence of DCMU + hydroxylamine and found equal to 0.60. We thus obtain $0.975 \times 0.6 = 0.585$.

disproves Dekker's suggestion [8] of a Q_A^- contamination in these spectra. The absence of a discernible oscillation at 550 nm suggests that, at this wavelength, the change on the first flash is due entirely to the Q_A^- of inactive centers. It is worth noting that we obtained similar results with BBY particles concerning the presence of a period 4 oscillation at 540 nm and its absence at 550 nm. However, a significant difference with algae is the superimposition of a period 2 contribution at these wavelengths, agreeing with the finding by Schatz and Van Gorkom [16] that a small C-550 change is associated with the Q_B^--Q_B spectrum in BBY's. By contrast, no influence of the secondary acceptor state is detectable in *C. sorokiniana*.

Using the 550 nm calibration and the (295 nm)/(550 nm) ratio from the DCMU spectrum of Fig. 2, we can thus estimate the contribution of inactive centers on the first flash in the 295 nm sequence plotted in the right-hand figure. This is shown by the downward arrow that falls reasonably close to the first flash value predicted from a deconvolution of the sequence from the second flash on (see the legend). The magnitude of the contribution from inactive centers, as estimated through the 550 nm change, was found identical irrespective of the preillumination procedure used for modulating the initial S_0/S_1 distribution (not shown). This supports the validity of the deconvolution technique used in Ref. 6, where this constancy had been assumed. As was stressed in that paper and in other ones [5,7], the absorption change on the first flash is lower in S_0-rich than in S_1-rich sequences (see Figs. 4, 6–7 in the present paper). This was used as a qualitative indication that the extinction coefficient of $S_0 \rightarrow S_1$ was smaller than that of $S_1 \rightarrow S_2$. A possible fallacy in this argument could arise from (i) a dependence of FF on preillumination, or (ii) an anomalous dark-adapted state in the S_0-rich sequence, such as presence of an 'S_{-1}' state. Possibility (i) is not supported by the present results; (ii) will be examined later when discussing Fig. 6.

An additional cross-check can be found by using the spectrum of the $S_1 \rightarrow S_2$ transition obtained independently. This may be done, as previously described [17], by subtracting the (Q_A^--Q_A) contribution from the $S_2Q_A^-$ spectrum (with DCMU) of Fig. 2. The former change is obtained in the presence of both DCMU and hydroxylamine that replaces the OEC as a donor to PS II, normalizing both spectra at 550 nm. In order to estimate the contribution of $S_1 \rightarrow S_2$ on the first flash of the sequence, one needs again a calibration wavelength, now indicating the amount of *active* centers. The field-indicating change (peaking at 511 nm in S-56), expressing the amount of charge separation carried out by PS II centers, can be used to that end. The 511 nm changes caused upon each flash at 75 μs were plotted in the left-hand part of Fig. 3. A step decrease is observed between the first and second flash, followed by a linear decrease, in agreement with the 550 nm information. The 511 nm signal on the second flash can be used as an indicator of the amount of oxygen-evolving centers. If one neglects the fraction of centers initially in state S_0 in the one flash preilluminated sequence of Fig. 3, one can predict the 295 nm change on the first flash due to the $S_1 \rightarrow S_2$ transition (see legend for details). The result is shown by the upward

arrow, that is again reasonably close to the value (open circle) deduced from the deconvolution of the rest of the sequence. By contrast, a poorer fit is obtained on the first (and some other) flashes by assuming the 1, 1, 1, −3 pattern for the extinction coefficients of the S-transitions (open squares, using a normalization on the third flash).

One may remark that the progressive decrease of active centers expressed by the slope of the 550 nm and 511 nm sequences (left-hand panel) should cause a systematic bias in the deconvolution. As shown elsewhere [18,19], this process does not correspond to a gradual increase of the miss coefficient during the sequence, but to a progressive withdrawal of centers that abruptly stop contributing the oscillating pattern. The 511 nm indicator can thus be used to correct the 295 nm sequence by renormalizing it to a constant number of active centers. When this is done (not shown), slightly smaller damping parameters are obtained and the relative magnitudes of the deconvoluted extinction coefficients remain similar (0.159, 0.649 and 0.506 instead of, respectively, 0.080, 0.586 and 0.510). The first flash change predicted from these parameters is slightly larger than obtained from the uncorrected sequence and lies still closer to the estimates shown by the dashed arrows.

Testing the preillumination / deactivation procedures

I will now describe methodological tests using spinach BBY particles. In order to estimate reliably the dark distribution of the S_0 and S_1 states, it is most useful to modulate this initial state through flash preillumination. This approach was however questioned by Dekker [8], who suggested that a 'phase shift' could be present in preilluminated sequences, expressing a deactivation pathway towards S_0 instead of S_1, or even the presence of a fraction of centers in an 'S_{-1}' state. Such anomalies could be due to the use of FCCP that was added for shortening the deactivation time. This substance was also used in the present experiments, but at a much lower concentration than in our previous work (2 nM instead of 500 nM), in order to avoid significant deactivation (and cytochrome *b*-559 oxidation) during the sequences. In the presence of 2 nM FCCP, a dark time of 4 mn was found sufficient for complete deactivation of states S_2 and S_3 in BBY's. Panels A and B in Fig. 4 compare sequences of absorption changes at 295 nm, in the presence (open circles) and absence (solid circles) of FCCP. No preillumination was given in A, while a three-flash preillumination was given in B, with a deactivation time of 13 mn (no FCCP) or 4 mn (with FCCP). As may be seen, FCCP caused little effect in the dark-adapted sequence, while the slightly larger deviations in the preilluminated sequence may be ascribed either to incomplete deactivation of the sample in the absence of FCCP or to

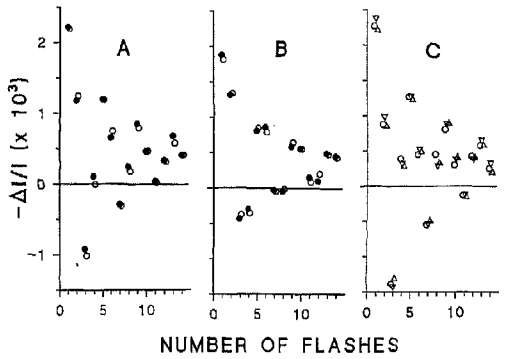

Fig. 4. Sequences of absorption changes at 290 nm in BBY's during series of flashes spaced 1 s apart. The absorption was sampled in the 850 ms–1 s range after each flash and plotted with respect to the level preceding the flash. DCBQ was present at a concentration of 25 μM. The solid circles in A and B were obtained in the absence of FCCP, the open circles and the data of panel C in the presence of 2 nm FCCP. Panel A: non preilluminated sample. Panel B preillumination by a group of three flashes followed by a deactivation period of 13 mn (without FCCP) or 4 mn (with FCCP). Panel C: sequences recorded after various preillumination procedures; 1 flash, 4 min darkness (circles); 3 flashes, 4 min, 1 flash, 4 min (downward-pointing triangle); 3 flashes, 4 min, 2 flashes, 4 min (upward-pointing triangles). The symbols were shifted horizontally for clarity (also in Figs. 3, 6 and 7).

interference of the $S_0Y_D^+ \rightarrow S_1Y_D$ reaction [20,21] due to the longer dark time. Measurements at 559 nm in the presence of 2 nM FCCP (not shown) revealed no detectable photo-oxidation of cytochrome *b*-559. From these tests, we conclude that a low concentration of FCCP can be safely used, causing no significant distortion of the sequences.

Panel C in Fig. 4 compares sequences resulting from three preillumination procedures in the presence of FCCP. In the sequence shown with circles, one preflash was given, followed by 4 mn deactivation. In the other sequences, the preillumination consisted of a first group of three flashes followed by 4 mn deactivation and one flash (downward-pointing triangles) or a group of two flashes (upward-pointing triangles), followed by a second deactivation period of 4 mn. All three procedures are expected to result in an initial state esentially composed of S_1 (> 96%), if complete deactivation has been achieved during the dark periods and if the S_2 and S_3 states deactivate only towards S_1 (not towards S_0). The similarity of the sequences supports these assumptions. One may first notice that an increase in the S_1 content has been achieved with respect to the unpreilluminated sequence (panel A), as may be inferred from the larger negative change on the third flash and positive change on the fourth one. A second remark is that if there were a significant deactivation probability of S_2 deactivating towards S_0, then the 1 F sequence in which a large transient population of S_2 has occurred should differ from the 3 F/1 F

sequence where this population was much lower. A third remark is that no 'S_{-1}' state is involved. If such a state had been populated in the 3 F pretreatment, one additional flash should restore the S_0 state and two flashes would be required to obtain a maximal amount of S_3: the similarity of the 3 F/1 F and 3 F/2 F sequences excludes this possibility to any significant extent. These tests show that no unwanted side-effect occurs in the preillumination/deactivation treatments, that can be used safely to predict or modulate the initial S_0/S_1 distribution.

Inactive centers in BBY's

As may be seen in the BBY sequences of Figs. 4, 6, 7 – and confirmed by the deconvolution work – the change on the first flash is larger than expected from an extrapolation of the subsequent oscillating pattern, suggesting the presence of inactive centers in BBY particles as well as in algae. The finding in this material of an additional absorption change on the first flash was already reported by Dekker et al. [4]. The presence of inactive PS II centers was confirmed by the detection (not shown) of a step increase of the C-550 change on the first flash, similarly to the S-56 experiments described earlier. The occurrence of inactive PS II centers in preparations of granal membranes (BBY's), to a similar extent as found in thylakoids, does not support the view [22,23] that they reflect essentially centers from stromal membrane regions. Another discrepancy with previous reports [24,25] is that we did not observe any reactivation of these centers in the presence of DCBQ (even at high concentration, and using either the 2,5 or 2,6 forms). This result (J.L. and E. Leci, unpublished data) was found not only in BBY's, but also in algae (monitoring the C-550 or field-indicating changes – while DCBQ penetration was demonstrated from the enlargement of the acceptor pool) or pea and spinach thylakoids (monitoring fluorescence). As yet, we have no explanation for this disagreement with literature data. The restoration kinetics of the inactive centers after a flash in BBY's (not shown) was found to be slower ($t_{1/2} \approx 4.5$ s) than in intact material – and also the recombination kinetics of normal centers in the presence of DCMU ($t_{1/2} \approx 3$ s). Thus, there is little contribution of inactive centers beyond the first flash in our sequences, in spite of the 1 s spacing. Such a contribution would not distort the sequences, anyhow, being lumped in the constant offset extracted through the deconvolution.

Elimination of the semiquinone signal in BBY's

A prerequisite for obtaining spectra of the S-transitions is to design a reliable way of eliminating the oscillating contribution (periodicity of two flashes) arising from the Q_B two-electron gate on the acceptor side. The method used in Ref. 6 took advantage of the

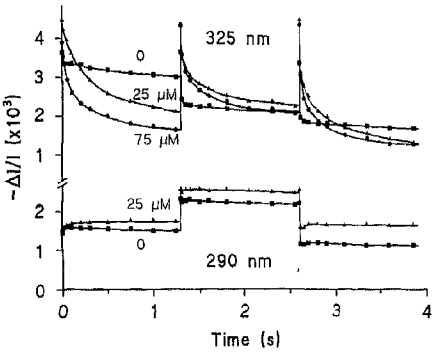

Fig. 5. Time-course of absorption changes at 290 nm and 325 nm in the absence or presence of DCBQ during a series of three flashes (triggered at times 0, 1.3 s and 2.6 s). Squares, no DCBQ; triangles, 25 μM DCBQ; circles, 75 μM DCBQ.The 75 μM data at 290 nm were close to the 25 μM curve and are omitted for clarity. The three first datapoints are at 1 ms, 10 ms and 50 ms after each flash.

stability of the semiquinone state Q_B^-. A preillumination with continuous light caused equipartition of the Q_B and Q_B^- states that was preserved during the FCCP-accelerated deactivation. This technique cannot be used in BBY's because the Q_B^- state is less stable, even in the absence of added acceptor. Furthermore, the endogenous pool of plastoquinone is diminished in these preparations, requiring addition of an acceptor such as DCBQ, that still accelerates Q_B^- reoxidation. Thus, another strategy may be using a high concentration of DCBQ so that complete reoxidation of Q_B^- occurs after each flash of the sequence. Fig. 5 (upper curves) shows the time course of absorption changes at 325 nm where both S-state and semiquinone changes contribute. When increasing the DCBQ concentration, the extent and rate of the semiquinone decay are increased. Using flashes spaced by more than 1 s, the presence of a periodicity of 2 flashes in the decay becomes undetectable at concentrations above 75 μM DCBQ. A drawback of using high DCBQ concentrations is a degradation of the samples activity during dark incubation (half-time around 90 mn), accompanied by an increase of background absorbance in the UV, probably due to degradation of the quinone. A slight increase of the miss coefficient was also observed. Therefore, we used samples to which DCBQ had been freshly added, discarding them within less than 30 mn.

It is interesting to compare the effect of increasing DCBQ concentrations on the absorption changes at 325 nm and 290 nm. At 325 nm, one observes no global trend towards absorption increase (or decrease) during the course of a flash series, in agreement with detection at this wavelength of semiquinone form(s) that do not accumulate. At 290 nm, an isobestic wavelength for

plastosemiquinone formation, a global absorption increase occurs during the flash series in the absence of DCBQ, expressing plastoquinol accumulation. This trend is enhanced in the presence of DCBQ, showing that the quinol form of DCBQ is also absorbing at this wavelength, with larger extinction coefficient. However, in the presence of DCBQ, the semiquinone decay observed at 325 nm is not accompanied by a concomitant absorption increase at 290 nm (Fig. 5). The increase is actually occurring at shorter times (< 50 ms) after the flash and no further significant change is seen in the 100 ms time-range when the semiquinone disappears. This suggests that the semiquinone form monitored at 325 nm is now that of DCBQ which probably substitutes to plastoquinone for binding to the Q_B pocket, and that this species absorbs at 290 nm about as much as the quinol formed during its decay. The decay of the DCBQ semiquinone appears to occur through two competing processes. Firstly, the classical two-step reduction in the Q_B pocket that accounts for the rapid (10 ms) 325 nm absorption decrease on the second flash (see the [DCBQ] = 25 μM curve in Fig. 6). Secondly, the spontaneous decay in the 100 ms range that must correspond to a dismutation reaction. Interestingly, this pathway is accelerated when increasing the concentration of DCBQ, suggesting that free DCBQ (not bound to the Q_B pocket) is involved in this process, possibly through the presence of free semiquinone as reported in Ref. 26.

The practical conclusion of this study is that a satisfactory elimination of semiquinone binary oscillations is achieved when using DCBQ above ≈ 75 μM, with a flash spacing of 1 s or more. At wavelengths where this contribution is basically small, such as 290–295 nm, 25 μM DCBQ suffices to render it negligible (as in Figs. 4, 6), with the advantages of a greater stability of the material and also of a somewhat smaller miss coefficient in the sequences (the origin of this effect was not investigated). The routine conditions that we used otherwise for obtaining spectra of the S-transitions consisted of 150 μM DCBQ and a 1 s spacing between flashes. An additional safety measure in the elimination of binary oscillations resides in the differential method described below.

A differential deconvolution method

This method was designed to overcome two potential problems in the deconvolution of absorption changes associated with the S-state transitions. The first one is the possible persistence of slight semiquinone oscillations. The second one is the possible uncertainty in the determination of the initial amounts of S_0 (denoted σ) and S_1 $(1-\sigma)$ resulting from flash preilluminations. In both cases, arguments were given in the foregoing showing that these problems were actually avoided under our experimental conditions. Nevertheless, this method provides an interesting way of cross-checking these conclusions.

The sequence of absorption changes (Eqn. 4 in section Methods) depends on σ through the transition coefficients $T_i(n)$. Any particular sequence in dark-adapted material can be considered as being made up of two contributions: σ times the sequence starting with 100% S_0 and $(1-\sigma)$ times that starting with 100% S_1. Indicating the initial S_0 concentration by a superscript, one has:

$$\Delta A^{\sigma}(n) = \sigma \Delta A^{0}(n) + (1-\sigma)\Delta A^{1}(n) \tag{6}$$

Or, using Eqn. 4:

$$\Delta A^{\sigma}(n) = \sigma \sum_{i=0}^{2} e_i T_i^{0}(n) + (1-\sigma) \sum_{i=0}^{2} e_i T_i^{1}(n)$$

$$= \sigma \sum_{i=0}^{2} e_i (T_i^{0}(n) - T_i^{1}(n)) + \sum_{i=0}^{2} e_i T_i^{1}(n) \tag{7}$$

Now, suppose one has measured two sequences with different (but unknown) initial distribution, say σ and σ'. The difference between these sequences is:

$$\Delta A^{\sigma}(n) - \Delta A^{\sigma'}(n) = (\sigma - \sigma') \sum_{i=0}^{2} e_i (T_i^{0}(n) - T_i^{1}(n)) \tag{8}$$

This is a system with coefficients $(T_i^0(n) - T_i^1(n))$ that depend only upon α and β. Solving the system gives values of the unknowns $u_i = (\sigma - \sigma')e_i$. At this step we have obtained the *relative magnitudes* of the differential extinction coefficients. Plugging the values of the u_i terms in Eqn. 7, one has:

$$\Delta A^{\sigma}(n) = \sigma/(\sigma - \sigma') \sum_{i=0}^{2} u_i (T_i^{0}(n) - T_i^{1}(n))$$

$$+ 1/(\sigma - \sigma') \sum_{i=0}^{2} u_i T_i^{1}(n) \tag{9}$$

in which $\sigma/(\sigma - \sigma')$ and $1/(\sigma - \sigma')$ are the only unknowns left. Solving Eqn. 9 – two flashes suffice in principle – gives the values of these unknowns and thus of σ and σ'.

To summarize, it suffices to have two sequences of S-state related absorption changes (or any S-related signal, really) with different σ values: then the individual extinction coefficients and values of σ in both sequences can be computed. The only requirement is to know the values of α and β, that can be estimated from any sequence including at least seven flashes, as explained in the Methods section. An additional advantage in this method is that the first step, solving system (8) to obtain the u_i terms does not require using pure S-dependent sequences: any two sequences will

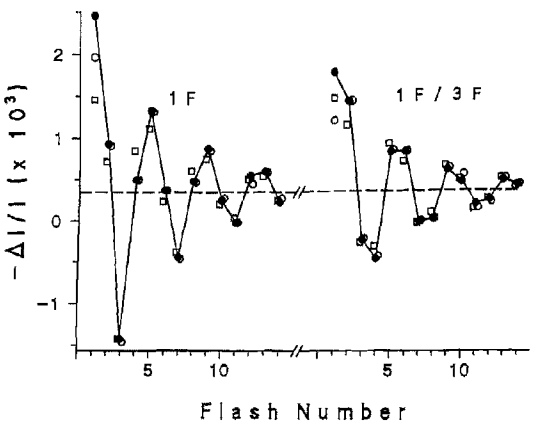

Fig. 6. Absorption changes at 290 nm during a series of flashes (solid circles) with the same timing as in Fig. 4. DCBQ was present at a concentration of 25 μM. Left: 1 flash preillumination, 4 min deactivation. Right: 1 flash, 4 min, 3 flashes, 4 min. The data are those of Table I, (b) and (c) respectively. The open circles show the simulated sequences obtained with the deconvoluted parameters given in line 1 of the Table. The dashed line indicates the SS level. The squares show the simulated sequences obtained with the 1, 1, 1, −3 model with normalization on the third flash of the 1 F sequence, using the same Kok parameters and SS level.

do, provided the extraneous contribution cancels when taking the difference. Thus the data may contain an additional binary oscillation arising from the acceptor side: provided this interfering contribution is identical in both sequences, the *relative* magnitudes of the extinction coefficients can still be obtained. It then suffices to run the same experiment at a wavelength where the interference is negligible (e.g., 290 nm) to obtain the σ values and thus to achieve the computation of the absolute e_i values. A word should be added concerning the presence of a constant offset upon each flash (steady-state level, denoted SS), corresponding here to accumulation of the quinol form of DCBQ. This contribution is easily dealt with by introducing a fourth unknown 'e' in the equations with a constant $T(n)$ coefficient: the minimum number of equations is then four instead of three.

Deconvolution tests at 290 nm

Table I gives raw data from an experiment in which BBY's were used in their native dark-adapted state (a), or preilluminated as follows: one flash (b), one flash/three flashes (c), or three flashes (d), implying a 4 mn deactivation period after each group of flashes. Sequences (b) and (c) have been plotted in Fig. 6. In the bottom part of Table I are given results from various deconvolution procedures. In all cases the first flash was discarded. The first four lines were obtained from the difference method described above, using the various couples combining an S_1-rich and S_0-rich sequence. Line 5 was obtained by ordinary deconvolution (i.e., solving system (4)) of sequence (b), assuming $\sigma = 0.02$ as expected from the preillumination procedure. Clearly, a satisfactory cross-check emerges from the comparison. The difference method yields σ values of −0.03 and 0.00 for (b), 0.07 and 0.11 for (a), 0.55

TABLE I

Illustration of various deconvolution treatments

The top panel gives raw data at 290 nm for a batch submitted to various preilluminations (sequences b and c are shown in Fig. 6). The bottom panel gives deconvoluted parameters for this experiment (lines 1–5) and for the 295 nm experiment shown in Fig. 7. Line 6 refers to the 1 s absorbance changes, line 7 to the ms-phase sequences. The change on the first flash was not used in any of the treatments. α and β were averaged from the individual values obtained on all sequences (a–d for lines 1–5 and the four sequences of Fig. 7 for lines 6–7; the standard deviation was very small in each case). When the difference method was used (all lines except 5), σ_1 refers to the S_1-rich sequence, σ_2 to the S_0-rich one. The steady-state level (SS) was treated as a common unknown in both sequences of the couple (except in line 5). In line 5, σ was estimated a priori, using α, β and assuming $\sigma = 0.25$ in the unpreilluminated state. The absorbance changes (top) and extinction coefficients (bottom) are given in units of $-\Delta I/I = 10^{-3}$.

	Flash number											
	1	2	3	4	5	6	7	8	9	10	11	12
(a) 0F	2.410	1.071	−1.229	0.271	1.192	0.516	−0.394	0.344	0.781	0.374	0.011	0.367
(b) 1F	2.456	0.926	−1.424	0.496	1.320	0.370	−0.445	0.476	0.866	0.240	−0.024	0.535
(c) 1F/3F	1.766	1.422	−0.241	−0.470	0.815	0.816	−0.020	0.011	0.595	0.452	0.186	0.237
(d) 3F	1.741	1.346	−0.299	−0.391	0.771	0.786	0.002	−0.012	0.609	0.505	0.139	0.166

	α	β	σ_1	σ_2	e_0	e_1	e_2	SS
1 (b)–(c)	0.066	0.099	0.00	0.57	0.113	1.609	1.250	0.342
2 (b)–(d)	0.066	0.099	−0.03	0.54	0.010	1.556	1.260	0.338
3 (a)–(c)	0.066	0.099	0.11	0.55	0.075	1.516	1.414	0.334
4 (a)–(d)	0.066	0.099	0.07	0.52	−0.060	1.454	1.430	0.329
5 (b)	0.066	0.099	(0.02)	–	0.170	1.639	1.228	0.356
6	0.054	0.079	0.03	0.64	0.213	1.841	1.048	0.493
7	0.054	0.079	−0.03	0.64	−0.428	−0.684	−0.713	0.779

and 0.57 for (c), 0.52 and 0.54 for (d). If one had arbitrarily taken 0.25 for the non preilluminated state, one would have predicted 0.02 for (b) and, from this value, 0.56 for (c). Thus, measurement of σ by the difference method supports the validity of a priori predictions from the preillumination procedures. Besides, the e_i values obtained by the different methods are similar – and also agree with the results previously obtained with algae [6] (see also Fig. 3 above). The direct deconvolution of line 5, not using the difference method, also yields similar results. It should be stressed that, although the fit of the data from individual experiments is generally very good (see Figs. 6 and 7), a significant scatter of the deconvolution results was nevertheless observed. This sensitivity to small experimental inaccuracies may not be surprising if one recalls that 7 parameters at least are involved (the three Kok parameters, the three e terms and SS). The results of Table I are thus meant as a methodological illustration, while more accurate estimates of the e values were obtained (Figs. 8, 9) by averaging on a number of experiments.

The open circles in Fig. 6 show the computed values using the results of line 1. The computed values for the first flash – that was not used in the deconvolution – suggest a similar contribution of inactive centers to both sequences, as could be expected. This does not support the suggestion [8] that the $S_0 \rightarrow S_1$ transition (largely contributing the first flash change in the right-hand sequence) could have distinct spectral properties when starting from a 'relaxed' S_0 state reached during dark-adaptation. The square symbols in Fig. 6 were computed from Dekker's (1, 1, 1, −3) model, taking the same Kok parameters and normalizing on the third flash change of the left-hand sequence.

The millisecond phase of the absorption changes

As originally pointed out by Velthuys [27], the amplitude of the absorption decay in the millisecond range following each flash, in a region where the acceptor side does not interfere, should behave, at least approximately, as an oxygen-evolution sequence. Indeed, the $S_iY_Z^+ \rightarrow S_{i+1}Y_Z$ reactions (where Y_Z denotes the secondary tyrosine donor mediating oxidation of the S-states) all occur in the range of a few 100 μs, with the exception of $S_3Y_Z^+ \rightarrow S_0Y_Z + O_2$, which is about 10-fold slower. Therefore the amplitude of the ms-phase should predominantly indicate the $S_3Y_Z^+ \rightarrow S_0Y_Z(+O_2)$ reaction. The similarity found by Dekker [8] and Van Leeuwen et al. [9] between the pattern of changes associated with the S-transitions and that of the ms-phase amplitude was presented as an argument in support of the 1, 1, 1, −3 pattern. Indeed, as previously pointed out [5], there is a direct proportionality relation between the oxygen sequence and the

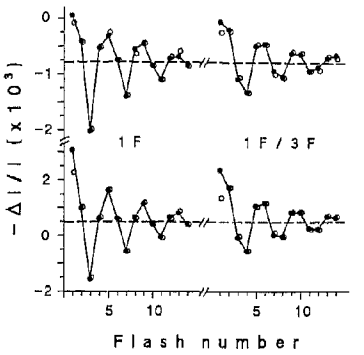

Fig. 7. Absorption changes at 295 nm during a series of flashes (solid circles). DCBQ was present at a concentration of 25 μM. Same preillumination procedures as in Fig. 6. The bottom sequences show the absorption changes in the 850 ms-1 s range as in Figs. 4 and 6. The top sequences are a plot of the difference of the absorption levels at 10 ms minus 1 ms after each flash. The open circles show the computed sequences using the deconvolution parameters given in Table I, line 6 (bottom sequences) and 7 (top sequences). The dashed lines indicate the SS level in each case.

absorption changes of the S-transitions in the case of the 1, 1, 1, −3 model.

Fig. 7 shows a plot of the ms-phase amplitude at 295 nm (upper sequences) compared with the corresponding 1 s absorption changes (lower sequences), using the same preillumination procedures as in Fig. 6. The ms-amplitudes were taken as the difference between absorption changes at 10 ms minus 1 ms. At variance with Dekker and Van Gorkom, significant differences between both patterns are obvious when comparing the 1 F sequences. The ms-sequence looks more like an oxygen yield sequence starting from almost 100% S_1, with the fourth and fifth flash signals close to each other. Deconvolution results of the data of Fig. 7 are shown in Table I (lines 6 and 7), using the difference method, and the corresponding fits were plotted as open circles in the figure. The σ values computed either from the ms-phase sequences (line 6) or from the 1 s sequences are in good agreement (± 0.03) and compare well with those predicted from the preilluminations (0.01 and 0.67). The extinction coefficients found for the ms-phase in the successive transitions are −0.428, −0.684, −0.713 and 4.865. The fourth value, e_3 in our notation, was computed according to the relationship $e_3 = (4\ SS/(1-\alpha+\beta)) - (e_0 + e_1 + e_2)$, where SS is the steady-state level obtained from the deconvolution of the ms-phase sequences. Thus, taking the origin as $e_0 = 0$ and normalizing at 100 on e_3, we have a pattern like 0, −5, −5, 100 instead of the pure oxygen pattern 0, 0, 0, 100. This slight discrepancy is not unexpected, since the contribution of the $S_iY_Z^+ \rightarrow S_{i+1}Y_Z$ reactions to the ms-phase should not be totally negligible on the second and third transitions: the half-times found for the four successive reactions by

Dekker and co-workers [28] were, respectively, 30, 110, 350 and 1300 μs.

The accordance of the ms-phase sequences with the expected pattern excludes a significant interference of the reduction reaction of S_2 or S_3 by Y_D during the 1 s interval between flashes. A similar conclusion may also be drawn from the 290 nm kinetics of Fig. 5, showing no decay reflecting deactivation in this time-range. Y_D denotes the tyrosine residue which is the counterpart in the D_2 protein of the secondary donor Y_Z in D_1. Its oxidation by S_2 or S_3 at pH 6.5 was reported to occur with $t_{1/2} = 4$ s [21], while its dark re-reduction occurs (in the presence of S_1) in the hours range. In our samples that were not submitted to prolonged dark-adaptation, Y_D remains presumably largely oxidized and, besides, the 1 s flashing interval would allow the reaction to proceed to less than 1/8th of its full extent. A possible complication could arise from the $S_0Y_D^+ \rightarrow S_1Y_D$ reaction. Vass and Styring [21] found a marked pH dependence for the rate of this reaction and reported a $t_{1/2} \approx 5$ min at pH 6.5. This process should tend to partially reset the 3-flash preilluminated sequences towards an S_1-rich state. However, a comparison of those sequences after 4 min (FCCP present) or 13 min (no FCCP) dark-adaptation (Fig. 4, panel B) indicates only a minor evolution in this direction. Besides, the values of σ actually *measured* by the difference method (see Table I) are close to those *predicted* when disregarding the $S_0Y_D^+ \rightarrow S_1Y_D$ reaction. They also agree with those that may be estimated from the 'oxygen-like' sequences of the ms-phase in Fig. 7. We thus conclude that the oxidation reaction of S_0 by Y_D^+ is slower under our conditions than found by Vass and Styring. Finally, it may be emphasized again that the deconvolution results that we obtained in the 290 nm region *do not require* the use of the 3-flash preilluminated sequences: similar extinction coefficients are found when treating the sole S_1-rich sequence (line 5 in Table I).

Spectra of the S-transitions

The following procedure was used, based on the tests detailed in the foregoing. For measurements at each wavelength, a fraction was taken from a common dark-adapted BBY pool and used for less than 30 mn after adding 150 μM DCBQ and 2 nM FCCP. Typically five wavelengths were investigated using a given pool, including 290 nm (on the third fraction). At each wavelength two types of sequence were recorded (averaging 2 to 6 runs according to the noise conditions): a non-preilluminated sequence and a 3-flash preilluminated sequence (after 4 mn deactivation). The sequences obtained in this manner are somewhat less contrasted in σ than sequences (b) and (c) in Table I, but this minimizes the deactivation periods and the overall duration of the experiment. The data were first used for determining α and β and then treated by the difference method (solving Eqn. 8 using all flashes but the first one). The σ values determined by solving Eqn. 9 at 290 nm (where absence of binary interference is warranted) were used to recover the absolute values of the extinction coefficients at other wavelengths. This overall procedure was repeated so as to have 4 to 10 experiments at each wavelength (and of course many more at 290 nm) and the deconvoluted coefficients were finally averaged. The resulting spectra are shown in Figs. 8 and 9.

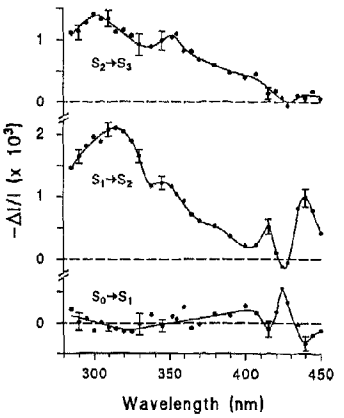

Fig. 8. Spectra of the S-transitions obtained as described in the text (not corrected for flattening). Some error bars are given that were computed from the scatter of individual experiments ($\pm 0.66 \times$ S.D.).

The main features that were found in previous work with algae [6] are confirmed in the present results: the $S_0 \rightarrow S_1$ spectrum is close to zero in the whole UV region (290–380 nm), the $S_1 \rightarrow S_2$ and $S_2 \rightarrow S_3$ spectra

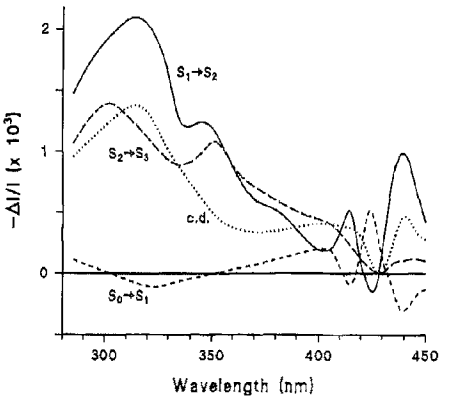

Fig. 9. Spectra of the S-transitions obtained by replotting the curves of Fig. 8. The dotted line (c.d.) shows the $S_2 \rightarrow S_3$ spectrum in Ca^{2+}-depleted material [17]. According to the estimate given in Ref. 17, one unit of the ordinate scale corresponds to an absorbance of 4.17 mM^{-1} cm^{-1} (neglecting the small flattening factor occurring in BBY's).

are significantly different, the latter being smaller in the peak region, with an overall larger bandwidth. It should be stressed that, besides the biological material, the methods used in both investigations were essentially different. This concerns for instance the procedure used for eliminating semiquinone signals, the use in the present study of a very low concentration of FCCP (shown not to affect the sequences, or to cause *b*-559 oxidation, in any detectable way). This holds also for the deconvolution procedure: the change on the first flash was not used here, and the σ's were experimentally measured instead of guessed from preillumination procedure. This agreement between largely independent techniques, and also the various cross-checks that were reported in the foregoing should leave little room for a significant bias in these results, insofar as the presumably oversimple Kok model to which the data were fitted is valid. What is meant here is that some dependence of α and β on the individual S-transitions may be expected [30]. However, from measurements of the extent of charge separation $(1 - \alpha + \beta)$ upon each flash of a series through the electrochromic field indicating absorption change (see the 511 nm data in Fig. 3), it turns out that this dependence cannot be very pronounced. Thus, while further refinements are certainly possible, they should not affect the present results drastically.

Compared with the earlier results, the spectra of Fig. 9 present a significantly improved resolution. Several features are now clearly apparent. A shoulder around 350 nm is seen in the $S_1 \rightarrow S_2$ change, which was already reported by Dekker et al. [6] and also found in the DCMU ± hydroxylamine spectrum shown in Ref. 17. A secondary peak in the same region is also now resolved in the $S_2 \rightarrow S_3$ spectrum that was first drawn as a broad shapeless band in Ref. 6. Significant improvement is also obtained in the blue region (400–450 nm) where interference from cytochrome *b*-559 was degrading the accuracy in our previous work. This perturbation is totally absent here and the presence of an electrochromic shift on $S_0 \rightarrow S_1$, inverted with respect to $S_1 \rightarrow S_2$, is now clearly established. I will now discuss the interpretation of these spectra.

The interpretation of the multiline EPR signal associated with S_2 (see reviews [2,3]) suggests that the $S_1 \rightarrow S_2$ transition corresponds to an Mn(III) to Mn(IV) oxidation within the Mn cluster. This is supported by X-ray absorption studies [31], and the UV absorption change is also consistent with this identification. Indeed, similar changes, due to metal-to-ligand charge transfer bands, have been observed in model Mn compounds [32,33]. The absence of any significant absorption change for the $S_0 \rightarrow S_1$ step in the same region suggests a markedly different process for this transition. There are indications from X-ray work [34] that a manganese oxidation is also involved in this case, although the present resolution of these experiments may not allow a firm conclusion. If such is indeed the case, the most plausible hypothesis accounting for the optical results would probably be an Mn(II) → Mn(III) transition (as concluded from X-ray spectroscopy [34]) that may be expected to show a charge transfer band at shorter wavelengths in the UV (although this is not a strict rule, see Ref. 33). The recent conclusion from X-ray spectroscopy [35] (see also Ref. 36) that the S_1 state includes only Mn(III) also supports rejection of an Mn(III) → Mn(IV) reaction upon $S_0 \rightarrow S_1$.

In contrast with the first transitions, the X-ray spectroscopy results have been consistently interpreted as excluding a manganese oxidation on the $S_2 \rightarrow S_3$ step [31,37]. A similar conclusion was also drawn from NMR [38] and EPR [39] relaxation studies. Additional support in that direction has been obtained in a system modified through calcium depletion in the presence of EGTA [17]. Under such conditions the system can be photo-converted to a formal S_3 state, but does not undergo further oxidation towards S_4. This modified S_3 gives rise to a new EPR signal [40] which cannot be ascribed to Mn oxidation, but may be simulated by interaction of an organic radical ($g = 2$) with the Mn cluster [17]. The optical spectrum associated with formation of this state (replotted as a dotted line in Fig. 9) was shown [17] to be very similar to that of the OH-adduct radical of histidine (imidazole) described in pulse radiolysis experiments [41]. Therefore, we proposed that the modified S_3 state corresponded to formation of this radical and envisaged extension of this identification to the normal system. Comparing the $S_2 \rightarrow S_3$ spectrum of the modified system with that of the functional one (Fig. 9), it appears that the shape and amplitude are similar in the 290–330 nm region, while the secondary peak around 350 nm is absent in the modified system (and in the in vitro spectrum of the oxidized histidine radical). An additional difference is also seen in the blue region where no electrochromic shift occurs on $S_2 \rightarrow S_3$, while such a shift was present in the modified system, suggesting the absence of deprotonation in the latter case. At the present stage, we can only propose several hypotheses. A first possibility is that the S_3 state covers a redox equilibrium between two species. The 305 nm peak could correspond to an OH adduct of histidine and the 350 nm peak to another oxidized species (which we call X). Although the 350 nm shoulder of the $S_1 \rightarrow S_2$ spectrum may be, coincidentally, a feature of the Mn spectrum, it could alternatively be explained by a partial oxidation of X in the S_2 state, through a redox equilibrium with Mn(IV). An extension of this hypothesis would exclude histidine oxidation in the normal system and ascribe the 305 nm band to Mn(IV): state S_3 would correspond to total oxidation of the Mn-X couple that was half oxidized in S_2 (this would imply that the X-ray experiments were

not accurate enough to detect partial Mn oxidation on the $S_2 \rightarrow S_3$ step). A second possibility is an all-histidine hypothesis for the $S_2 \rightarrow S_3$ spectrum, which would ascribe both the 305 and 350 nm bands to this radical in the normal system, assuming that local interactions in situ might account for this difference with the in vitro spectrum, or that of the Ca-depleted system. A third possibility is ascribing the whole $S_2 \rightarrow S_3$ spectrum to a non-histidine radical. A plausible candidate is tryptophan (indole). Pulse radiolysis experiments [42] have established the spectrum of the OH-adduct that displays a major peak at 307 nm and secondary ones at 326 nm and 346 nm. These various peaks were ascribed to different sites for OH binding on the indole ring. Thus the $S_2 \rightarrow S_3$ spectrum could express such a radical with OH distributed between the two locations corresponding to the 307 and 346 nm peaks. Alternatively, an indole radical with attachement of OH at a single site (346 nm peak) may be proposed for X in the first hypothesis.

The involvement of an OH adduct of an aromatic residue as an intermediate step in water oxidation is an attractive possibility. In pulse radiolysis experiments, the OH radical readily reacts with the aromatic ring. In the oxygen-evolving system, the adduct could result from stabilization of the cationic amino-acid radical through binding of OH^-. Involvement of an OH radical as an intermediate in photosynthetic water oxidation has generally been rejected on thermodynamic grounds, although Renger [43] suggested that a large association constant could provide the required energy. Formation of a covalent OH adduct may indeed be considered as a case of high binding energy in which the radical character is supported mostly by the amino-acid ring. Consistent with this hypothesis is the neutral character of the $S_2 \rightarrow S_3$ reaction as seen from the absence of electrochromic effect and from proton release measurements (in the pH 5.5 to 8 range) that are reported elsewhere [29].

The band-shift observed in the blue region (and also in the red) has been ascribed [4,44,45] to a local electrochromic influence of the charged S-states on a neighboring chlorophyll *a* molecule, possibly P-680. This change is observed both on the $S_1 \rightarrow S_2$ step and, with smaller amplitude and inverted direction, on $S_0 \rightarrow S_1$. The classical 1,0,1,2 pattern for proton release from the S-transitions [46–48] would predict a net charge increase on the $S_1 \rightarrow S_2$ transition where no proton is released. This would account for the electrochromic change observed on this step, but not for the opposite change reported here for $S_0 \rightarrow S_1$. In recent work, we re-investigated the proton release pattern as revealed by experiments with Neutral Red. This led to the proposal of a modified, non-integer stoichiometry [49,50], that was further confirmed by a detailed study of proton release in BBY's, as a function of pH [29]. Proton release on $S_2 \rightarrow S_3$ remained close to 1, while the stoichiometry was found to vary between pH 5.5 and 8 from (respectively) 1.7 to 1 for $S_0 \rightarrow S_1$ and 0 to 0.5 for $S_1 \rightarrow S_2$. Thus, at pH 6.5 (as in the present experiments), more than one proton (≈ 1.3) is released upon $S_0 \rightarrow S_1$ and less than one (≈ 0.15) upon $S_1 \rightarrow S_2$. The first transition thus results in a *negative* net charge that accounts for the observed electrochromic effect.

Acknowledgements

The author is indebted to Prof. G. Babcock, particularly for suggesting the possibility of a secondary peak in the $S_2 \rightarrow S_3$ spectrum and for introduction to the art of BBY's. Helpful interaction with F. Rappaport and stimulating discussions with Drs. J. Dekker, A. Boussac and W. Rutherford are also gratefully acknowledged. This work was supported by the Centre National de la Recherche Scientifique.

References

1 Joliot, P. and Kok, B. (1975) in Bioenergetics of Photosynthesis (Govindjee, ed.), pp. 387–412, Academic Press, New York.
2 Rutherford, A.W. (1989) Trends Biochem. Sci. 14, 227–232.
3 Babcock, G.T., Barry, B.A., Debus, R.J., Hoganson, C.W., Atamian, M., McIntosh, L., Sithole, I. and Yokum, C.F. (1989) Biochemistry 28, 9557–9565.
4 Dekker, J.P., Van Gorkom, H.J., Wensink, J. and Ouwehand, L. (1984) Biochim. Biophys. Acta 767, 1–9.
5 Lavergne, J. (1986) Photochem. Photobiol. 43, 311–317.
6 Lavergne, J. (1987) Biochim. Biophys. Acta 894, 91–107.
7 Lavergne, J. (1989) Photochem. Photobiol. 50, 235–241.
8 Dekker, J.P. (1991) in Manganese Redox Enzymes (Pecoraro, V.L., ed.), VDL publications. New York, in press.
9 Van Leeuwen, P.J., Vos, M.H. and Van Gorkom, H.J. (1990) Biochim. Biophys. Acta 1018, 173–176.
10 Berthold, D.A., Babcock, G.T. and Yocum, C.F. (1981) FEBS Lett. 131, 231–234.
11 Joliot, P., Béal, D. and Frilley, B. (1980) J. Chim. Phys. 77, 209–216.
12 Joliot, P. and Joliot, A. (1984) Biochim. Biophys. Acta 765, 210–218.
13 Lavorel, J. (1978) J. Theor. Biol. 57, 171–185.
14 Chylla, R., Garab, G. and Whitmarsh, J. (1987) in Progress in Photosynthesis Research (Biggins, J., ed.), Vol. II, pp. 237–240, Martinus Nijhoff, Dordrecht.
15 Graan, T. and Ort, D.R. (1987) in Progress in Photosynthesis Research, (Biggins, J., ed.), Vol. II, pp. 241–244, Martinus Nijhoff, Dordrecht.
16 Schatz, G.H. and Van Gorkom, H.J. (1985) Biochim. Biophys. Acta 810, 283–294.
17 Boussac, A., Zimmermann, J.-L., Rutherford, A.W. and Lavergne, J. (1990) Nature 347, 6290, 303–306.
18 Joliot, P., Lavergne J. and Béal, D. (1989) in Current Research in Photosynthesis (Baltscheffsky M., ed.), Vol. II, pp. 879–882, Kluwer, Dordrecht.
19 Lavergne, J. and Joliot, P. (1991) Trends Biochem. Sci. 16, 129–134.
20 Styring, S. and Rutherford, A.W. (1987) Biochemistry 26, 2401–2405.

21 Vass, I. and Styring, S. (1991) Biochemistry 30, 830–839.
22 Guenther, J.E. and Melis, A. (1990) Photosynth. Res. 23, 105–109.
23 Henrysson, T. and Sundby, C. (1990) Photosynth. Res. 25, 107–117.
24 Graan, T. and Ort, D.R. (1986) Biochim. Biophys. Acta 852, 320–330.
25 Cao, J. and Govindjee (1990) Biochim. Biophys. Acta 1015, 180–188.
26 Hoganson, C.W. and Babcock, G.T. (1988) Biochemistry 27, 5848–5855.
27 Velthuys, B.R. (1981) in Photosynthesis (Akoyunoglou, G., ed.), Vol. II, pp. 75–85, Balaban International Science Services, Philadelphia.
28 Dekker, J.P., Plijter, J.J. Ouwehand, L. and Van Gorkom, H.J. (1984) Biochim. Biophys. Acta 767, 176–179.
29 Rappaport, F. and Lavergne, J. (1991) Biochemistry, in press.
30 Bouges-Bocquet, B. (1980) Biochim. Biophys. Acta 594, 85–103.
31 Goodin, D.B., Yachandra, V.K., Britt, R.D., Sauer, K. and Klein, M.P. (1984) Biochim. Biophys. Acta 767, 209–216.
32 Bodini, M.E., Willis, L.A., Riechel, T.L. and Sawyer, D.T. (1976) Inorg. Chem. 15, 1538–1543.
33 Vincent, J.B. and Christou, G. (1986) FEBS Lett. 207, 250–252.
34 Guiles, R.D., Yachandra, V.K., McDermott, A.E., Cole, J.L., Dexheimer, S.L., Britt, R.D., Sauer, K. and Klein, M.P. (1990) Biochemistry 29, 486–496.
35 Kusunoki, M., Ono, T., Matsushita, T., Oyanagi, H. and Inoue, Y. (1990) J. Biochem. 108, 560–567.
36 Nishida, Y. and Nasu, M. (1990) Z. Naturforsch. 45c, 1004–1010.
37 Guiles, R.D., Zimmermann, J.-L., McDermott, A.E., Yachandra, V.K., Cole, J.L., Dexheimer, S.L., Britt, R.D., Wieghardt, K., Bossek, U., Sauer, K. and Klein, M.P. (1990) Biochemistry 29, 471–485.
38 Srinivasan, A.N. and Sharp, R.R. (1986) Biochim. Biophys. Acta 851, 369–376.
39 Styring, S. and Rutherford, A.W. (1988) Biochemistry 27, 4915–4923.
40 Boussac, A., Zimmermann, J.-L. and Rutherford, A.W. (1989) Biochemistry 28, 8984–8989.
41 Rao, P.S., Simic, M. and Hayon, E.J. (1975) J. Phys. Chem. 79, 1260–1263.
42 Armstrong, R.C. and Swallow, A.J. (1969) Radiat. Res. 40, 563–579.
43 Renger, G. (1978) in Photosynthetic Water Oxidation (Metzner, H., ed.), pp. 229–248, Academic Press, London.
44 Saygin, O. and Witt, H.T. (1985) FEBS Lett. 187, 224–226.
45 Velthuys, B.R. (1988) Biochim. Biophys. Acta 933, 249–257.
46 Fowler, C.F. (1977) Biochim. Biophys. Acta 462, 414–421.
47 Saphon, S. and Crofts, A.R. (1977) Z. Naturforsch. 32c, 617–626.
48 Förster, V. and Junge, W. (1985) Photochem. Photobiol. 41, 183–190.
49 Lavergne, J. and Rappaport, F. (1990) in Current Research in Photosynthesis (Baltscheffsky, M., ed.), Vol. I, pp. 873–876, Kluwer, Dordrecht.
50 Jahns, P., Lavergne, J., Rappaport, F. and Junge, W. (1991) Biochim. Biophys. Acta 1057, 313–319.